Modes of oscillation in radiofrequency Paul traps

2012 New J. Phys. 14 093023

(http://iopscience.iop.org/1367-2630/14/9/093023)

New Journal of Physics
The open-access journal for physics

Modes of oscillation in radiofrequency Paul traps

H Landa[1,5], M Drewsen[2], B Reznik[1] and A Retzker[3,4]

[1] School of Physics and Astronomy, Raymond and Beverly Sackler Faculty of Exact Sciences, Tel-Aviv University, Tel-Aviv 69978, Israel
[2] Department of Physics and Astronomy, QUANTOP, Danish National Research Foundation Center for Quantum Optics, University of Aarhus, DK-8000 Århus C, Denmark
[3] Institut für Theoretische Physik, Universität Ulm, D-89069 Ulm, Germany
[4] Racah Institute of Physics, The Hebrew University of Jerusalem, Jerusalem 91904, Israel
E-mail: haggaila@gmail.com

New Journal of Physics **14** (2012) 093023 (21pp)
Received 20 June 2012
Published 13 September 2012
Online at http://www.njp.org/
doi:10.1088/1367-2630/14/9/093023

Abstract. We examine the time-dependent dynamics of ion crystals in radiofrequency traps. The problem of stable trapping of general three-dimensional crystals is considered and the validity of the pseudopotential approximation is discussed. We analytically derive the micromotion amplitude of the ions, rigorously proving well-known experimental observations. We use a recently proposed method to find the modes that diagonalize the linearized time-dependent dynamical problem. This allows one to obtain explicitly the ('Floquet–Lyapunov') transformation to coordinates of decoupled linear oscillators. We demonstrate the utility of the method by analyzing the modes of a small 'peculiar' crystal in a linear Paul trap. The calculations can be readily generalized to multispecies ion crystals in general multipole traps, and time-dependent quantum wavefunctions of ion oscillations in such traps can be obtained.

[5] Author to whom any correspondence should be addressed.

Contents

1. Introduction

The trapping of charged particles by electromagnetic fields is an essential tool for many investigations within physics [1, 2] and chemistry [3, 4], as well as for studies of biomolecules [5, 6]. In the Paul trap, charged particles are confined by oscillating multipole radiofrequency (rf) fields [3]. Different types of Paul traps have been proposed and constructed over the years, and an increasing number of experimental and theoretical works are dedicated to the improvement of these devices (see, e.g., [7]). With the advent of laser-cooling techniques [8], a great deal of effort has been focused on the study of crystalline forms of trapped ions [9–37]. Single trapped ions have been cooled to the quantum ground state of motion [38, 39], and crystals of a few ions have been cooled to the ground state in at least a few of the motional modes [40]. Long-range order has been observed with large structures of thousands of ions in Penning [21, 22] and Paul traps [37, 41].

In this paper, we analyze the dynamics of crystals of charged particles confined in rf traps. In section 2, we review some previous results on the trapping of ions in rf traps. In section 3, we discuss the linear stability of ion crystals in general, and consider the limits of validity of the pseudopotential (time-independent) approximation, in relation to symmetries of the trapped crystal. We derive the micromotion amplitude of ions in a general periodic solution in a Paul trap, and relate our findings to recent experimental results. We then expand the motion of the trapped ions in coordinates of small displacements about the periodic solution, which is the dynamic equivalent of a minimum of the trapping potential. This expansion is completely general and can be applied to any periodic trapping field. In section 4, we solve the coupled motion of the ions in the time-dependent potential. We find the modes that diagonalize the dynamical problem and explicitly obtain a time-dependent transformation to coordinates in which the motion is that of decoupled linear oscillators. Using this expansion the exact time-dependent wavefunctions of ions in rf traps can be obtained. In section 5 we present our

numerical study of a small crystal in a linear Paul trap, and conclude the paper in section 6 with comments on directions for further applications and research.

2. Overview of Paul trapping

The first crystallization of a cloud of charged aluminum microparticles has been reported in [42]. Wigner crystals of 2 to approximately 100 trapped ions in a Paul trap were reported in [9, 10] and further investigated in [43] both experimentally and numerically. The simulations included rf trapping, Coulomb interaction, laser cooling and random noise. Depending on trap parameters, the ions were found to equilibrate either as an apparently chaotic cloud or in an ordered structure. The latter is defined as the 'crystal' solution when it is a simple limit cycle, with the ions oscillating at the rf frequency about well-defined average points. The transition between the two phases has been investigated, it was shown that both phases can coexist and hysteresis in the transition has been observed [43].

The motion of two ions in the Paul trap has been investigated in detail in various publications [44–53]. In addition to the aforementioned phases, frequency-locked periodic attractors (where the nonlinearity pulls the motional frequencies into integral fractions of the external rf frequency) were found in numerical simulations and experiments. These solutions are different from the crystal in that the ions move in extended (closed) orbits in the trap, whose period is a given multiple of the rf period. However, many of these frequency-locked solutions are unstable, especially those of a large period, and perturbations such as those coming from the nonlinearity of the laser-cooling mechanism tend to destroy them.

Despite the large amplitude motion, the frequency-locked solutions, being periodic, are of course not chaotic. However, even in the presence of cooling, some solutions in the ion trap may behave chaotically for exponentially long times. The authors of [54] suggest that, *eventually*, all trajectories settle at frequency-locked attractors, at least for two ions at $a = 0$. Numerical simulations and experiments with more ions suggest that, in general, different types of solutions—of chaotic and of long-range order nature—can coexist at the same parameter values [43].

A further important property of two-ion crystals was discovered in [55]. The entire first Mathieu stability zone (which corresponds to stable trapping of one ion) was mapped using numerical simulations to determine the stability of the two-ion crystal. It turned out that the Coulomb interaction destabilizes completely the two-ion crystal in some parameter areas. About one year later, it was independently discovered in [56–58] that two ions in a hyperbolic Paul trap may crystallize in a 'peculiar' crystal.

The reason why such crystals were termed 'peculiar' is that for a two-ion crystal with no angular momentum about the axial x-axis, there are only two possibilities in the harmonic pseudopotential approximation (excluding the case of degenerate secular frequencies). The crystal can either align with the x-axis or lie in the y–z plane. In the latter case we may assume that the crystal is aligned with the y-axis, and in both cases the z coordinate can be eliminated. Therefore a crystal that is at an angle to both the reduced axes x and y, i.e. one which forms an angle with both the axial axis and the plane of symmetry, is peculiar.

In [56, 57], an improved pseudopotential approximation was derived for two ions in the hyperbolic Paul trap (and in [59] for the linear Paul trap). This nonlinear pseudopotential can be used to derive approximately the areas of stability in parameter space of the axial and radial

two-ion crystals, and the orientation of the peculiar crystal. However, even the improved nonlinear pseudopotential cannot reproduce the areas of unstable crystal.

As mentioned above, the crystal solution in all these works is taken to be a periodic solution of the equations of motion with a period equal to that of the rf potential. This is a limit cycle of the equations, the simplest of the frequency-locked solutions mentioned above, and it is an attractive one when cooling is present and it is stable. Its stability is analyzed in [58] by looking at the Poincaré map associated with this solution. The Poincaré map is a mapping of the phase space onto itself, in which every initial point $\{x(0), p(0)\}$ is evolved according to the equations of motion and mapped to $\{x(T), p(T)\}$ after one rf period T. The crystal is by definition a fixed point of the Poincaré map, and its linear stability is determined by the linearized dynamics in its vicinity, specifically by the eigenvalues of the so-called monodromy matrix. The linearization takes into account the leading (harmonic) coupling between the ions, expanded about the periodic solution. Further analysis (both linear and nonlinear) of the periodic orbit of two ions in a Paul trap can be found in [60–63].

3. Paul traps

3.1. The trapping potential

We start with the potential energy of identical ions in the most general single, nonsegmented quadrupole rf trap. By choosing a specific frequency $\bar{\omega}$, which is characteristic of the secular frequencies in the problem, and measuring the time and distances in units of $1/\bar{\omega}$ and $d = \left(e^2/m\bar{\omega}^2\right)^{1/3}$, respectively (with m and e the ion's mass and charge), we write the nondimensional potential as

$$V = V_{\text{trap}} + V_{\text{Coulomb}} = \sum_i^N \frac{1}{2}\left(\Lambda_x x_i^2 + \Lambda_y y_i^2 + \Lambda_z z_i^2\right) + \sum_{i\neq j} \frac{1}{2}\|\vec{R}_i - \vec{R}_j\|^{-1}, \tag{1}$$

where $\vec{R}_i = \{x_i, y_i, z_i\}$ is the vector coordinate of ion i, the trapping terms are given by $\Lambda_\alpha = \frac{\Omega^2}{4}(a_\alpha - 2q_\alpha \cos\Omega t)$, $\alpha \in \{x, y, z\}$, with a_α and q_α being the nondimensional Mathieu parameters of the respective coordinates [64] and Ω being the rf frequency (in units of $\bar{\omega}$).

Regarding the trapping parameters, the Laplace equation implies that

$$\sum_\alpha a_\alpha = \sum_\alpha q_\alpha = 0. \tag{2}$$

Two commonly used types of traps are the hyperbolic [65] and linear [64] Paul traps. Taking the x-axis as the axial direction, the hyperbolic trap can be described by setting $a_y = a_z \equiv a$, $a_x = -2a$ and $q_y = q_z \equiv q$, $q_x = -2q$, while in the linear trap we have $a_y = a_z \equiv a$, $a_x = -2a$ and $q_y = -q_z \equiv q$, $q_x = 0$ (so a must be negative to obtain stable trapping). In the next subsection, we will relate to the symmetries of these two trapping geometries, but for now we keep the discussion completely general.

The trapping potential V_{trap} when considered alone gives rise to decoupled Mathieu equations in each ion coordinate [66]. The corresponding characteristic exponents are $\beta_\alpha(a_\alpha, q_\alpha)$ and the secular frequencies are then $\omega_\alpha \equiv \beta_\alpha \frac{\Omega}{2}$. In the units being used, V_{trap} and V_{Coulomb} are both of the order of unity for a crystal when the trapping balances the Coulomb repulsion. These units allow naturally the introduction of the parameter

$$\epsilon \equiv 4/\Omega^2. \tag{3}$$

If $\bar{\omega}$ is the (dimensional) secular frequency along some specific axis α, we have $\omega_\alpha = 1$ and $\epsilon = \beta_\alpha^2$. Using the familiar lowest order approximation [64], $\beta_\alpha \approx \sqrt{a_\alpha + q_\alpha^2/2}$, we see that the limit $\epsilon \to 0$ is equivalent to $a_\alpha \to 0$, $q_\alpha^2 \to 0$. This parameter will be used in the following.

When the Mathieu parameters belong to a single-particle stability zone, the potential of equation (1) allows for bounded motion and large ion clouds can be trapped for extraordinarily long times without cooling. This is given by the limit $\vec{R}_i \to \infty$ in equation (1), which means that ions are not crystallized, rather their motion is that of decoupled trapped particles. Despite the large amplitude motion, at low enough density the ions hardly interact.

However, stable single-particle parameters do not guarantee that a stable crystal solution exists, even with two ions, as discussed extensively in section 2, which has also been recently investigated with crystals consisting of up to several hundreds of ions [67, 68]. We recall that a stable crystal solution is considered as a periodic solution with the same period of the rf, which is linearly stable under small perturbations. The existence of a stable crystal solution is a property of the fully nonlinear and time-dependent problem. There may also exist stable multi-periodic solutions (with a period that is some large, arbitrary multiple of the rf period), the frequency-locked solutions described in section 2.

In experiments, even in the presence of cooling, crystals may exist only metastably, changing completely after a given time or when parts of the crystal are moving with respect to the rest [37]. In this case, if the timescale of the change of the crystal is long enough, the analysis in the following subsections, using modes expanded about the (quasi-) periodic solution, may still be useful, even though at least one mode would be unstable.

3.2. Linearization using the pseudopotential modes

In this subsection we linearize the crystal motion using the pseudopotential modes. Therefore this treatment assumes that a crystal solution exists, and is close to the crystal of the pseudopotential. As is known from the example of two ions in a hyperbolic Paul trap, this assumption may not hold even for arbitrarily small values of a and q (where the crystal is 'peculiar' [56–58]). The linearized secular modes of a one-dimensional Coulomb chain were treated in detail in [69–71].

Let us define the squared ratio of secular radial and axial frequencies $\gamma_y = \omega_y^2/\omega_x^2$, $\gamma_z = \omega_z^2/\omega_x^2$ and $\gamma_x = \omega_x^2/\omega_x^2 = 1$, thus choosing $\bar{\omega}$ as the axial trapping frequency, so we can rewrite the potential as the sum $V = V_{\text{pseudo}} + V_{\text{Coulomb}} + V_{\text{rf}}$,

$$V = \sum_{i,\alpha}^{N} \frac{1}{2}\gamma_\alpha (\vec{R}_{i,\alpha})^2 + \sum_{i \neq j} \frac{1}{2} \| \vec{R}_i - \vec{R}_j \|^{-1} + \sum_{i,\alpha}^{N} \frac{1}{2}(\Lambda_\alpha - \gamma_\alpha)(\vec{R}_{i,\alpha})^2. \tag{4}$$

We expand about the minimum-configuration locations, $\{\vec{R}_i^0\}$, obtained from the secular part of V in equation (4), $V_{\text{pseudo}} + V_{\text{Coulomb}}$, and change to the normal modes Θ_j by setting

$$\vec{R}_{i,\alpha}(t) = \vec{R}_{i,\alpha}^0 + \sum_{j}^{3N} D_{i,\alpha}^j \Theta_j(t), \tag{5}$$

where $D_{i,\alpha}^j$ is the matrix of normal mode vectors, with rows indexed by the N ion numbers i and three directions α and columns by the $3N$ normal mode numbers j. Writing the potential

in terms of the normal modes, $V = V_{\text{harmonic}} + V_{\text{rf}} + V_{\text{nonlinear}}$, we keep only the first two terms to obtain

$$V = \sum_i \frac{1}{2}\omega_i^2 \Theta_i^2 + \sum_{i,\alpha}^{N} \frac{1}{2}\left(\Lambda_\alpha - \gamma_\alpha\right)\left(\vec{R}^0_{i,\alpha} + \sum_j^{3N} D^j_{i,\alpha}\Theta_j\right)^2 + \cdots \tag{6}$$

and the linearized equation of motion (e.o.m.) derived from equation (6) is

$$\ddot{\Theta}_m + \omega_m^2 \Theta_m = -\frac{\partial V_{\text{rf}}}{\partial \Theta_m} = -\sum_{i,\alpha}^{N}\left(\Lambda_\alpha - \gamma_\alpha\right) D^m_{i,\alpha}\left(\vec{R}^0_{i,\alpha} + \sum_j^{3N} D^j_{i,\alpha}\Theta_j\right). \tag{7}$$

Before treating the coupled system described by equation (7), we first note that when the rf trapping potential is symmetric with respect to the axes of symmetry of the crystal, the equations of motion are in fact diagonal. For the following few paragraphs, let us therefore limit the discussion to the hyperbolic and the linear Paul traps, whose parameters were described following equation (2). Given these two trapping geometries, the current expansion will be diagonal if the crystal is two dimensional and lies in the plane of cylindrical symmetry of a hyperbolic trap, or the crystal is one dimensional and aligned with one of the trap axes, in either the hyperbolic or the linear trap. In that case, we have $\vec{R}^0_{i,\alpha} = 0$ for the coordinates transverse to the crystal, and also the normal modes decouple in these directions from the modes tangential to the crystal (i.e. $D^j_{i,\alpha}$ is divided into blocks in the index α).

We then can use two relations which hold in the plane of the crystal or along its axis,

$$\sum_{i,\tilde{\alpha}} D^m_{i,\tilde{\alpha}} D^j_{i,\tilde{\alpha}} = \delta_{mj}, \quad \sum_{i,\tilde{\alpha}} D^m_{i,\tilde{\alpha}} \vec{R}^0_{i,\tilde{\alpha}} = \xi_b \delta_{mb}, \tag{8}$$

where hereafter, $\tilde{\alpha}$ runs on the symmetry directions, $\xi_b = \sqrt{\sum_{i,\tilde{\alpha}} (\vec{R}^0_{i,\tilde{\alpha}})^2}$ and b denotes the breathing mode. The identity on the left in equation (8) is the completeness of the normal modes along the symmetry directions. To obtain the second identity we use the fact that in a harmonic trap, the breathing mode vector is exactly proportional to the minimum-configuration locations $\vec{R}^0_{i,\alpha}$ of the pseudopotential (see, e.g., appendix B of [15]), so that $D^b_{i,\tilde{\alpha}} = \vec{R}^0_{i,\tilde{\alpha}}/\xi_b$, and therefore the vector $\vec{R}^0_{i,\tilde{\alpha}}$ is orthogonal to all other normal mode vectors. By using equation (8) we can replace the rhs in equation (7) with the simple expression

$$-\frac{\partial V_{\text{rf}}}{\partial \Theta_m} = -\left(\Lambda_{\tilde{\alpha}} - \gamma_{\tilde{\alpha}}\right)\left(\xi_b \delta_{mb} + \Theta_m\right). \tag{9}$$

We find that the equations of motion for modes in the crystal plane or along its axis are, after multiplying by $\epsilon = 4/\Omega^2$ of equation (3) and rescaling $t \to \Omega t/2$,

$$\ddot{\Theta}_m + \left[\epsilon\left(\omega_m^2 - \gamma\right) + (a - 2q\cos 2t)\right]\Theta_m = \left[\epsilon\gamma - (a - 2q\cos 2t)\right]\xi_b \delta_{mb}, \tag{10}$$

where γ, a and q are defined along the symmetry axes. Similar equations hold in the directions transverse to the crystal, without the inhomogeneous rhs and with the corresponding γ, a and q.

Equation (10) shows explicitly how the isotropy of the potential along the axes of symmetry of the crystal allows us to decouple the equations of the modes. This decoupling puts the conditions for linear stability of the crystal in terms of diagonal Mathieu equations for each of the modes. In addition, with this symmetry the only mode with an inhomogeneous rhs is

the breathing mode, i.e. it is the only mode on which the rf potential acts as a driving force. This driven motion is, in fact, the π-periodic motion of the crystal as a whole, about the static minimum-configuration locations of the pseudopotential, $\{\vec{R}_i^0\}$.

Returning to the case of a general trap, in order to put equation (7) in a simple form we multiply it by $\epsilon = 4/\Omega^2$ of equation (3) and rescale $t \to \Omega t/2$. Defining the two matrices

$$A_{mj} = \epsilon\omega_m^2\delta_{mj} + \sum_{i,\alpha} D_{i,\alpha}^m D_{i,\alpha}^j (a_\alpha - \epsilon\gamma_\alpha), \qquad Q_{mj} = \sum_{i,\alpha} D_{i,\alpha}^m D_{i,\alpha}^j q_\alpha \tag{11}$$

and the vectors

$$G_m = -\sum_{i,\alpha} D_{i,\alpha}^m \, (a_\alpha - \epsilon\gamma_\alpha) \, \vec{R}_{i,\alpha}^0, \qquad F_m = \sum_{i,\alpha} D_{i,\alpha}^m q_\alpha \vec{R}_{i,\alpha}^0, \tag{12}$$

we rewrite equation (7) in vector notation as

$$\ddot{\vec{\Theta}} + [A - 2Q\cos 2t]\,\vec{\Theta} = \vec{G} + 2\vec{F}\cos 2t. \tag{13}$$

We solve the homogeneous lhs of equation (13) in section 4. Since the pseudopotential modes are expanded about static configuration points, equation (13) is an inhomogeneous equation with a π-periodic rhs, which has a unique π-periodic solution (except for possibly a region of measure zero in a_α, q_α space). This periodic solution of driven motion of the normal modes corresponds to the exact π-periodic solution which defines the crystal in the rf trapping potential. Details of the solution of the inhomogeneous equation can be found in [72].

Equation (13) shows that, in general, the rf couples the pseudopotential normal modes and also acts as a driving force. Under this coupling, the true modes of oscillation of the system may, in general, have different frequencies (and even lose stability), and different oscillation directions than the pseudopotential modes upon which this expansion is based. Indeed, the linearization starting from the pseudopotential approximation may not be adequate in the general case. We further investigate this point in the following two subsections.

3.3. The periodic crystal solution

We now abandon the pseudopotential approximation and turn to studying the time-dependent potential directly. In this subsection, we derive analytically the micromotion amplitude of the ions in typical crystals in Paul traps. The e.o.m. for the ion coordinates, derived from equation (1) after rescaling by $t \to \Omega t/2$, is

$$\ddot{\vec{R}}_{i,\alpha} + (a_\alpha - 2q_\alpha\cos 2t)\,\vec{R}_{i,\alpha} - \epsilon\sum_{\substack{j=1\\ j\neq i}}^{N} \|\vec{R}_i - \vec{R}_j\|^{-3}(\vec{R}_{i,\alpha} - \vec{R}_{j,\alpha}) = 0. \tag{14}$$

Equation (14) has π-periodic coefficients and is time-reversal invariant. We assume the existence of a crystal in the sense of section 2, i.e. a π-periodic and time-reversal invariant solution, which obtains the general form

$$\vec{R}_{i,\alpha}^{\pi}(t) = \sum_{n=-\infty}^{n=\infty} \vec{B}_{2n,i,\alpha}\, \mathrm{e}^{\mathrm{i}2nt}. \tag{15}$$

In this form, the average ion location is $\vec{B}_{0,i}$ (which is different from $\vec{R}_i^{\pi}$ $(t=0)$).

We now wish to see what can be said about $\vec{R}_i^{\pi}$ in typical Paul trapping experiments. We first define the dynamic matrix

$$G_{ij}(\{\vec{R}_i(t)\}) = \delta_{ij} \sum_{\substack{m \\ m \neq i}} \|\vec{R}_i - \vec{R}_m\|^{-3} - (1-\delta_{ij})\|\vec{R}_i - \vec{R}_j\|^{-3} \tag{16}$$

and write using equation (15) its Taylor and Fourier expansion around $\{\vec{B}_{0,i} - \vec{B}_{0,j}\}$ as

$$G_{ij} = G_{0,ij}(\{\vec{B}_{0,i}\}) + G_{2,ij}(\{\vec{B}_{0,i}\}, \{\vec{B}_{2,i}\})(\mathrm{e}^{2\mathrm{i}t} + \mathrm{e}^{-2\mathrm{i}t}) + \cdots . \tag{17}$$

Substituting the solution ansatz equation (15) into equation (14), we obtain

$$\sum_n \left[\left(a_\alpha - (2n)^2\right) \vec{B}_{2n,i,\alpha} - q_\alpha \left(\vec{B}_{2n-2,i,\alpha} + \vec{B}_{2n+2,i,\alpha} \right) - \epsilon \sum_j G_{ij} \vec{B}_{2n,j,\alpha} \right] \mathrm{e}^{\mathrm{i}2nt} = 0. \tag{18}$$

We replace $G_{ij}(\{\vec{R}_i(t)\})$ in equation (18) by its leading order, time-independent term from equation (17), $G_{0,ij} = G_{ij}(\{\vec{B}_{0,i}\})$, and require that the above relation holds for every t. We obtain, by using $\vec{B}_{2n} = \vec{B}_{-2n}$ and neglecting $\vec{B}_{4n} \approx 0$ (which is of the next order in q_α), the equation coming from the $n = 0$ term,

$$a_\alpha \vec{B}_{0,i,\alpha} - 2q_\alpha \vec{B}_{2,i,\alpha} - \epsilon \sum_j G_{0,ij} \vec{B}_{0,j,\alpha} = 0, \tag{19}$$

and the coupled equation from the coefficient of $\mathrm{e}^{2\mathrm{i}t}$,

$$(a_\alpha - 4)\, \vec{B}_{2,i,\alpha} - q_\alpha \vec{B}_{0,i,\alpha} - \epsilon \sum_j G_{0,ij} \vec{B}_{2,j,\alpha} = 0. \tag{20}$$

This system of equations can be seen as a linear homogeneous system in the $2N$ variables $\{\vec{B}_{0,i,\alpha}, \vec{B}_{2,i,\alpha}\}$, $i = 1, \ldots, N$, for fixed α, since the equations are diagonal along the three different axes. Of course, this is not really a linear system since the matrix $G_{0,ij}$ depends on $\vec{B}_{0,i}$, but since we are not trying to actually solve the system, this will not matter. Let us fix the index α to some axis (suppressing it in the following), and define the N-component vectors $\vec{u}_{0,i} = \vec{B}_{0,i,\alpha}$ and $\vec{u}_{2,i} = \vec{B}_{2,i,\alpha}$. Then the above system can be written in the block-matrix form

$$\begin{pmatrix} a - \epsilon G_0 & -2q \\ -q & -4 \end{pmatrix} \begin{pmatrix} \vec{u}_0 \\ \vec{u}_2 \end{pmatrix} = 0, \tag{21}$$

where we have neglected $a - \epsilon G_0$ as compared with -4 in the lower-right block of equation (21). Since we assume that the system has a solution (which approximates the π-periodic crystal), the above matrix must be singular. We can expand its determinant

$$0 = \det\left[a - \epsilon G_0 - (-2q)\,(-4)^{-1}\,(-q)\right] = \det\left[a - \epsilon G_0 + q^2/2\right]. \tag{22}$$

Taking $\vec{u}_0$ to be the vector from the kernel of $(a - \epsilon G_0 + q^2/2)$ which obeys $(a - \epsilon G_0)\vec{u}_0 = -(q^2/2)\vec{u}_0$, we find that the solution of equation (21) is $\vec{u}_2 = -\,(q/4)\,\vec{u}_0$.

We therefore have obtained that in a general quadrupole trap, in the π-periodic crystal solution of equation (15), every ion coordinate obeys (at least to leading order in $a_\alpha/4, q_\alpha/4, \epsilon_\alpha/4$)

$$\vec{B}_{2,i,\alpha} \approx -\frac{q_\alpha}{4} \vec{B}_{0,i,\alpha}, \tag{23}$$

i.e. that the micromotion amplitude in each coordinate is $q_\alpha/2$ of the respective average position, and at π phase with respect to the rf drive. In the hyperbolic trap the corresponding motion has been imaged as early as in [42]. In simulations of a generic trap (with different q and a parameters for the three axes), equation (23) seems to hold accurately to within a few per cent, for q up to $\sim$0.7, which is consistent with a deviation of order $(q_\alpha/4)^2$.

The relation in equation (23) loses its accuracy when either $\vec{B}_{0,i,\alpha} \ll 1$ or $q_\alpha \ll 1$. In the former case, for an ion near the zero of one of the rf axes, the corresponding micromotion amplitude, in fact, seems, in the cases we have checked, to be lower (this is similar to a single trapped ion at the origin of a Paul trap, for which the unique π-periodic solution is the trivial one).

For the linear Paul trap case of $q_\alpha \ll 1$ along the axial axis, the first-order expression in equation (23) loses its meaning. We must therefore add to equation (20) the second term in equation (17), $G_{2,ij}$, which rotates at the frequency e^{2it}. Setting $q = 0$, equation (21) is replaced with

$$\begin{pmatrix} a - \epsilon G_0 & 0 \\ -\epsilon G_2 & -4 \end{pmatrix} \begin{pmatrix} \vec{u}_0 \\ \vec{u}_2 \end{pmatrix} = 0. \tag{24}$$

We now examine what can be deduced about G_2. The off-diagonal elements are, in general,

$$G_{2,ij} = 3\|\vec{B}_{0,i} - \vec{B}_{0,j}\|^{-5} \sum_\alpha (\vec{B}_{0,i,\alpha} - \vec{B}_{0,j,\alpha})(\vec{B}_{2,i,\alpha} - \vec{B}_{2,j,\alpha}), \quad i \neq j. \tag{25}$$

In particular, using equation (23) with $q_y = -q_z = q$ and $q_x = 0$, we obtain that, for the linear Paul trap,

$$G_{2,ij} = -3\frac{q}{4}\|\vec{B}_{0,i} - \vec{B}_{0,j}\|^{-5}[(\vec{B}_{0,i,y} - \vec{B}_{0,j,y})^2 - (\vec{B}_{0,i,z} - \vec{B}_{0,j,z})^2] + O\left(\frac{q^2}{4^2}\right), \quad i \neq j. \tag{26}$$

Since the diagonal elements are the negative of the row sum, as in equation (16), $G_{2,ii} = -\sum_{m\neq i} G_{2,im}$, we immediately find that for a crystal which is invariant (up to a permutation of the ions) under $y \leftrightarrow \pm z$, $G_{2,ii} = 0 + O(q^2/4^2)$. In fact, for the linear Paul trap, the e.o.m., equation (14) is invariant under $y \leftrightarrow -z$, $t \to t + \pi/2$, so given one crystal solution, there is also a solution obtainable by an application of this transformation. Depending on the number of ions and trapping parameters, both solutions may actually be the same crystal. As the crystal size grows, by the same symmetry arguments, $G_{2,ii} \to 0 + O(q^2/4^2)$.

The second row of equation (24) gives $\vec{B}_{2,i,x} = -\epsilon/4 \sum G_{2,ij}\vec{B}_{0,j,x}$, and we argue that by the above symmetry arguments, for a typical symmetric or large crystal in a linear Paul trap, when the crystal configuration is also symmetric under $x \leftrightarrow -x$, the first-order terms in the above summation will cancel, and (using $\epsilon \approx q/2$)

$$\vec{B}_{2,i,x} = O\left(\frac{1}{2}\frac{q^3}{4^3}\right)\vec{B}_{0,i,x}. \tag{27}$$

If the symmetry alluded to above does not hold, equation (27) should be replaced with an expression which is one order less, namely $\vec{B}_{2,i,x} = O\left(\frac{\epsilon}{4}\frac{q}{4}\right)\vec{B}_{0,i,x}$.

Equation (27) explains why in the linear Paul trap, there is essentially no micromotion excitation along the axial direction despite the strong Coulomb interaction. In addition, since $q_y = -q_z$ in the linear trap, the oscillation described by equation (23) is exactly the (2,2) mode of cold-fluid theory [14], which has been observed both in simulations [20] and recently

discussed in connection with experiments [29]. In fact, in the simulations we have performed (section 5), equation (23) seems to hold extremely accurately radially (to within half a per cent), and equation (27) gives an accurate estimate for the axial micromotion amplitude (also matching, e.g., [20, 73]).

3.4. Linearization about the periodic crystal and the pseudopotential limit

In this subsection we expand the modes of oscillation of the ions about the periodic crystal solution, equation (15). The following expansion is applicable to general crystal configurations, does not rely on the pseudopotential modes or on a small parameter, and can be readily generalized to settings not considered in this paper, e.g. segmented traps and higher-order multipole traps. We will discuss its relation to the expansion of section 3.2, which used the pseudopotential modes.

Expanding the potential of equation (1) about the time-dependent solution $\{\vec{R}_i^{\pi}(t)\}$, in the coordinates of small oscillations $r_{i,\alpha} = \vec{R}_{i,\alpha} - \vec{R}_{i,\alpha}^{\pi}(t)$, and defining the π-periodic matrix

$$K_{ij}^{\sigma\tau}(t) = \left.\frac{\partial^2 V_{\text{Coulomb}}}{\partial R_{i,\sigma}\partial R_{j,\tau}}\right|_{\{\vec{R}_i^{\pi}(t)\}}, \tag{28}$$

we find the linearized e.o.m.

$$\ddot{r}_{i,\sigma} + (a_\sigma - 2q_\sigma \cos 2t)\, r_{i,\sigma} + \epsilon \sum_{j,\tau} K_{ij}^{\sigma\tau}(t)\, r_{j,\tau} = 0. \tag{29}$$

This equation is a linearly coupled system for the ion coordinates with π-periodic coefficients. We see that the interaction term in equation (29) is of the same order (in ϵ, or equivalently a and q^2) as the diagonal term. Expanding the matrix $K_{ij}^{\sigma\tau}(t)$ in a Fourier series in the form

$$K_{ij}^{\sigma\tau} = (K_0)_{ij}^{\sigma\tau} - 2\,(K_2)_{ij}^{\sigma\tau} \cos 2t - \cdots, \tag{30}$$

we first define the two matrices

$$A_{ij}^{\sigma\tau} = \delta_{ij}\delta_{\sigma\tau} a_\sigma + \epsilon (K_0)_{ij}^{\sigma\tau}, \quad Q_{ij}^{\sigma\tau} = \delta_{ij}\delta_{\sigma\tau} q_\sigma + \epsilon (K_2)_{ij}^{\sigma\tau}. \tag{31}$$

We can now switch the notation to a simpler one with dynamical variables u_m whose single index m stands for both indices $\{i, \sigma\}$ of $r_{i,\sigma}$, with the corresponding indices replaced in equation (31), and rewrite equation (29) in vector notation, with only the two leading harmonics of the Fourier series, as

$$\ddot{\vec{u}} + [A - 2Q\cos 2t]\,\vec{u} = 0. \tag{32}$$

This equation describes linearized coupled perturbations about the π-periodic solution which defines the crystal in the time-dependent potential. In section 4 we will solve this coupled system and find its decoupled modes of oscillation.

Equation (32) is seen to be identical in form to the lhs of equation (13), which is given in terms of the pseudopotential modes. However, the current expansion is based on the exact force acting between the ions during their motion along the periodic trajectory of the full potential. Higher harmonics from the Fourier series of this force can be added, and in section 5 we will in fact include the next harmonic ($\cos 4t$), to obtain very accurate results for the modes. When the nonlinear motion is not exactly π-periodic, some of the linearized modes of the above expansion may not be oscillatory (as detailed in section 4.1), which describes (locally) the aperiodic motion

of the crystal. If this change of the crystal is slow, the linearization of equation (29) can still be useful.

Considering the limit of taking the Mathieu parameters to zero, this does not guarantee that the crystal will be (linearly) stable. If there are unstable modes, they may remain unstable even as $a, q^2, \epsilon \to 0$. As for approaching the pseudopotential crystal in this limit, *if* the average ion locations $\{\vec{B}_{0,i}\}$ of the periodic solution tend to pseudopotential minimum locations, then the limit of the pseudopotential modes is regained on the lhs of equation (29). To characterize the conditions for this to occur, further investigations are required; however, for simple cases the results of section 3.3 may provide some hints.

In particular, if the rf potential is isotropic with respect to the configuration (as discussed in section 3.2 for specific cases), and we neglect K_2 in equation (31), the matrix Q becomes proportional to the identity. Then we can diagonalize equation (32) by an orthogonal transformation (which is exactly the transformation to the normal modes) and obtain equation (10). There will no longer be an inhomogeneous rhs, since the periodic crystal motion is already accounted for. In the presence of driven breathing oscillations, the ions feel stronger repulsive nonlinearity when they oscillate radially inwards, so we may expect the real crystal to be slightly more expanded (with the ion distances somewhat larger) as compared with the pseudopotential approximation.

We note that for an axial chain of ions in the linear Paul trap, indeed $K_2 \approx 0$ even if there is a small rf leak in the axial direction or if the ions do not lie exactly along the rf null axis, and equation (10) is almost exact. For the axial modes, the correction to the pseudopotential modes will be small. For the radial modes, the correction will typically be small, provided that the rf frequency is large compared with the radial frequencies. However, for calculation of small effects which might be of importance in high-accuracy experiments such as for quantum information processing [64], the full time-dependent solution must be used.

As a final note, a generalization of the isotropy of the rf potential with respect to the crystal configuration would be the existence of a constant orthogonal transformation which diagonalizes equation (32) and thus decouples the modes in the nonisotropic case. Such a transformation would simultaneously diagonalize the matrices A and Q (which must commute), and does not exist in the general case.

4. Solution of the linear equations

4.1. The Floquet problem

Equation (32) is a linear differential equation with periodic coefficients and therefore amenable to treatment using Floquet theory, which we briefly review here. For more details, see [72] and references therein. For the Newtonian problem with f degrees of freedom ($f = 3N$ for N ions in three dimensions), the corresponding Floquet problem is stated in terms of coordinates in $2f$-dimensional phase space by the definitions

$$\phi = \begin{pmatrix} \vec{u} \\ \dot{\vec{u}} \end{pmatrix}, \quad \Pi(t) = \begin{pmatrix} 0 & 1_f \\ -(A - 2Q\cos 2t) & 0 \end{pmatrix}, \tag{33}$$

where 1_f is the f-dimensional identity matrix. The e.o.m. is written in standard form as

$$\dot{\phi} = \Pi(t)\,\phi. \tag{34}$$

In the following, an f-dimensional vector $\vec{u}$ will be denoted by a lower case latin letter with an arrow. f-dimensional matrices will be denoted by capital latin letters (Q). A $2f$-dimensional vector ϕ will be denoted by a lower case greek letter. Capital greek letters (unitalicized) will denote $2f$-dimensional matrices (Π, B).

A fundamental matrix solution to equation (34) has $2f$ linearly independent column solutions and obeys the matrix equation $\dot{\Phi}(t) = \Pi(t)\Phi(t)$. A fundamental matrix solution that equals the identity matrix at $t = 0$, i.e. obeys $\Phi(0) = 1_{2f}$, is known as the *matrizant* of equation (34) (and is obviously unique). The matrizant can always be written in the form $\Phi(t) = \Gamma(t)\mathrm{e}^{\mathrm{B}t}\Gamma^{-1}(0)$, where $\Gamma(t+T) = \Gamma(t)$ is periodic with the period T of $\Pi(t)$, and the constant matrix B is diagonal, with entries known as the characteristic exponents of the Floquet problem,

$$\mathrm{B} = \mathrm{diag}\left\{\mathrm{i}\beta_1, \ldots, \mathrm{i}\beta_{2f}\right\}. \tag{35}$$

The time-dependent linear coordinate change, known as the 'Floquet–Lyapunov' transformation, defined by

$$\phi(t) = \Gamma(t)\chi(t), \tag{36}$$

transforms the e.o.m. equation (34) into the time-independent diagonal form

$$\dot{\chi} = \mathrm{B}\chi, \tag{37}$$

whose solutions are the Floquet modes,

$$\chi_\nu(t) = \chi_\nu(0)\mathrm{e}^{\mathrm{i}\beta_\nu t}. \tag{38}$$

We note that in the general case, Γ mixes the coordinates $\vec{u}$ and their derivatives, and in addition is not unitary, although certain highly symmetric cases, e.g. as those discussed in sections 3.2 and 3.4, when the Mathieu equations decouple completely, are an exception.

4.2. Solution using an expansion in infinite continued matrix inversions

We recently [72] proposed an analytical expansion of the solutions of the e.o.m. (32). This expansion allows one to obtain the frequencies and the coefficients of the solution vectors in a generalization of an infinite continued fractions expansion, to arbitrary precision. The solution is given in a form which is immediately suitable for obtaining the Floquet–Lyapunov transformation, as will be shown in the next subsection.

We seek the solutions of equation (32), in the form of a sum of two linearly independent complex columns vectors,

$$\vec{u} = \sum_{n=-\infty}^{n=\infty} \vec{C}_{2n}[b\,\mathrm{e}^{\mathrm{i}(2n+\beta)t} + c\,\mathrm{e}^{-\mathrm{i}(2n+\beta)t}], \tag{39}$$

where b and c are complex constants determined by the initial conditions. Stable modes will be described by β taking a real nonintegral value (we exclude the case of integral β). Following the discussion in section 4.70 of [66], for trapping parameters in the first stability zone of the Mathieu equation, β can be chosen in the range $0 < \beta < 1$ for all stable modes.

By defining $R_{2n} = A - (2n+\beta)^2$ we can write infinite recursion relations for $\vec{C}_{2n}$,

$$Q\vec{C}_{2n-2} = R_{2n}\vec{C}_{2n} - Q\vec{C}_{2n+2}, \tag{40}$$

and obtain two independent expansions in infinite continued matrix inversions

$$\vec{C}_2 = T_{2,\beta} Q \vec{C}_0 \equiv ([R_2 - Q[R_4 - Q[R_6 - \cdots]^{-1} Q]^{-1} Q]^{-1}) Q \vec{C}_0 \tag{41}$$

and

$$Q\vec{C}_2 = R_0 \vec{C}_0 - Q\vec{C}_{-2} = \tilde{T}_{0,\beta} \vec{C}_0 \equiv (R_0 - Q[R_{-2} - Q[R_{-4} - \cdots]^{-1} Q]^{-1} Q) \vec{C}_0. \tag{42}$$

Multiplying equation (41) by Q and defining

$$Y_{2,\beta} \equiv \tilde{T}_{0,\beta} - Q T_{2,\beta} Q, \tag{43}$$

we find that all characteristic exponents β are zeros of the determinant of $Y_{2,\beta}$ (which is a function of β). If there are degenerate β's they will appear as degenerate zeros of this determinant. The vector $\vec{C}_0$ for each β is an eigenvector of $Y_{2,\beta}$ with eigenvalue 0. Since A and Q are symmetric, $Y_{2,\beta}$ is symmetric as well, and so its kernel will be of dimension equal to the algebraic multiplicity of the β root. The vector $\vec{C}_2$ can be obtained by an application of $T_{2,\beta} Q$ to $\vec{C}_0$, for $n = -1$ we use $\vec{C}_{-2} = [T_{-2,\beta}]^{-1} Q \vec{C}_0$, and so on for the other vectors. We note that the different vectors $\vec{C}_{2n,\beta}$ are not orthogonal in general, and the vectors at every order in n mix different coordinates.

The general term of the expansion vanishes. Either A or Q may be singular and the expansion can still be applied in general. Even if both are singular, the expansion is valid if there are no integral values of β, a case that we do not tackle as noted above. Excluding perhaps isolated values of β (and atypically in the a–q parameter space), all matrices that are inverted in the above expressions will be invertible, and while employing the algorithm in practice, the invertibility of the matrices is, of course, easily verified at each step. In section 5 we use, in fact, a generalization of the above expansion [72] which includes also the next Fourier harmonic ($\cos 4t$, omitted from equation (30)).

4.3. The Floquet–Lyapunov transformation for stable modes

We now further assume that all Floquet modes are stable, i.e. that the $2f$ linearly independent solutions of equation (34) are oscillatory and thus come in complex conjugate pairs. This simplifies many expressions. We therefore take B of equation (35) in the block form

$$\mathrm{B} = \begin{pmatrix} \mathrm{i}B & 0 \\ 0 & -\mathrm{i}B \end{pmatrix}, \quad (B)_{f\times f} = \mathrm{diag}\{\beta_1, \ldots, \beta_f\}, \tag{44}$$

where β_j are positive. We define the f-dimensional matrix U whose columns are constructed from the series of f-dimensional vectors $\vec{C}_{2n,\beta_j}$ obtained from the recursion relations for the solutions of equation (39), i.e.

$$(U)_{f\times f} = \left(\sum \vec{C}_{2n,\beta_j} \mathrm{e}^{\mathrm{i}2nt} \ldots\right), \tag{45}$$

where in the above expression and for the rest of this section, the summation is over $n \in \mathbb{Z}$. We similarly define the f-dimensional matrix V composed of column vectors as

$$(V)_{f\times f} = \left(\mathrm{i}\sum \left(2n + \beta_j\right) \vec{C}_{2n,\beta_j} \mathrm{e}^{\mathrm{i}2nt} \ldots\right). \tag{46}$$

The matrices U and V can be chosen to obey the normalization condition

$$V^t\,(0)\,U\,(0) = \tfrac{1}{2}\mathrm{i}, \tag{47}$$

which is a rescaling imposed by multiplication with a (diagonal) matrix, such that

$$U \to U\left(-2\mathrm{i}V^t\,(0)\,U\,(0)\right)^{-\frac{1}{2}}, \tag{48}$$

and V accordingly. As shown in [72], the Floquet–Lyapunov transformation and its inverse can then be obtained in closed form, and are given block-wise by (where U^* denotes the complex conjugate of the matrix U),

$$\Gamma\,(t) = \begin{pmatrix} U & U^* \\ V & V^* \end{pmatrix}, \quad \Gamma^{-1}\,(t) = \begin{pmatrix} \mathrm{i}V^\dagger & -\mathrm{i}U^\dagger \\ -\mathrm{i}V^t & \mathrm{i}U^t \end{pmatrix}. \tag{49}$$

This transformation is a canonical transformation from the Hamiltonian coordinates $\vec{u}$ and their conjugate momenta $\vec{p} = \dot{\vec{u}}$, to the variables given by

$$\chi = \begin{pmatrix} \xi \\ \zeta \end{pmatrix},$$

where ξ is the new f-dimensional vector of coordinates and $-\mathrm{i}\zeta$ are the new conjugate momenta (we here break the notation a little). Using the realness of $\vec{u}$ and $\vec{p}$, it is easy to verify that $\xi = \zeta^*$. The time dependence of these modes is

$$\xi_j\,(t) = \xi_j\,(0)\,\mathrm{e}^{\mathrm{i}\beta_j t}, \quad \zeta_j\,(t) = \zeta_j\,(0)\,\mathrm{e}^{-\mathrm{i}\beta_j t}. \tag{50}$$

5. Computation of the modes of a 'peculiar' crystal

In figures 1–3 we consider a crystal of six ions, demonstrating the utility and generality of the analysis presented in this paper. The simulation is of an almost ideal linear Paul trap (with only a 1% DC asymmetry in the radial plane), such that the center-of-mass frequencies are degenerate to within 1%. The Mathieu parameters are $q_y = 0.41$ and $a_x = 0.05766$. In the pseudopotential approximation, the corresponding minimum configuration is a (nearly regular) octahedron, with two ions sitting on each axis of the trap. The rf crystal, on the other hand, may well deserve to be called 'peculiar' (in the sense described in section 2), since it is not oriented to the axes. There are two ions lying along the y-axis, along which the confinement is strongest, but the two other pairs of ions sit along lines which are rotated in the x–z plane. The large amplitude oscillation at the rf period, and the absence of micromotion along the axial direction, confirm very accurately the results presented in section 3.3.

Numerically, the periodic crystal solution can be obtained by starting from a simulation of the full e.o.m.'s with a friction (cooling) term and slowly turning it off (the adiabatic shutting down of the damping term is important). The crystal is then followed for a period and the periodic solution and force matrix can be Fourier expanded to obtain the matrices A and Q. Since the crystal is 'peculiar', it has no corresponding pseudopotential limit (normal modes of regular polyhederons were investigated in [74]; see also references cited in [75]). For a very accurate description of the modes in the Paul trap, we add to equation (32) the next Fourier harmonic to obtain $\ddot{\vec{u}} + [A - 2Q_2\cos 2t - 2Q_4\cos 4t]\,\vec{u} = 0$, and expand it in the method of continued matrix inversions, using the formulae given in appendix B of [72], which generalize the formulae presented in section 4. This modification is required in order to obtain accurately the low-frequency modes of nearly degenerate configurations, as in a peculiar crystal.

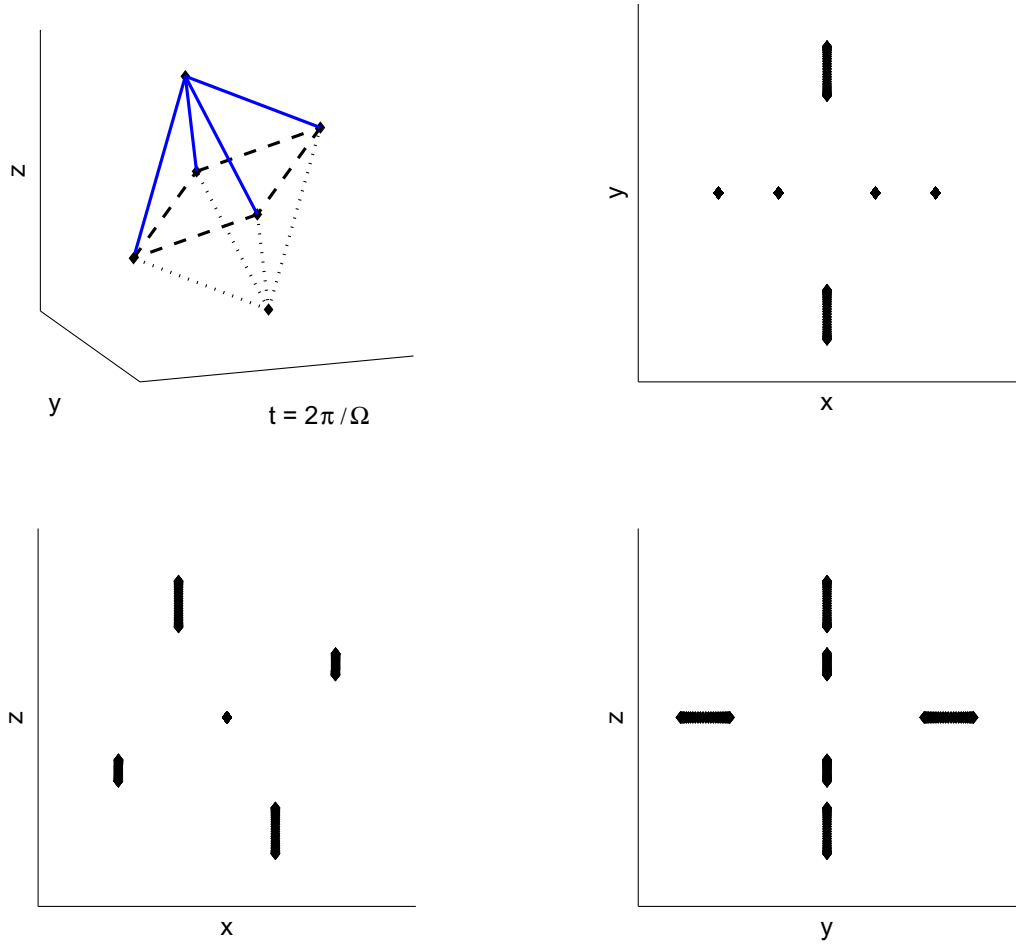

Figure 1. The periodic 'peculiar' crystal solution of six ions in a linear Paul at nearly spherical trapping parameters (see text for details). The average locations correspond to a (nearly regular) octahedron. Upper left: the ions at zero rf phase. The other three figures show the ion trajectories over one rf period. The oscillation with a large amplitude is given by equation (23) with an accuracy of 0.5%. The axial micromotion amplitude is of the order of 10^{-4} of the ions' radial positions (see section 3.3).

6. Concluding comments

In this paper we have investigated the dynamics of ion crystals in rf traps. We repeat the main results presented herein. In equation (7) we show that, in general, the rf couples the pseudopotential normal modes of the crystal and also acts as a driving force. For a crystal configuration that has the same symmetry as the trapping potential (e.g. a chain of ions or a planar crystal in a trap with cylindrical symmetry), we find that the equations of motion for the modes become decoupled Mathieu equations as in equation (10), for that the stability analysis is trivial (but may be different from the pseudopotential approximation).

In equations (23) and (27), we derive the results that have been observed in experiments and numerical simulations, namely that in a general ion crystal the micromotion amplitude in

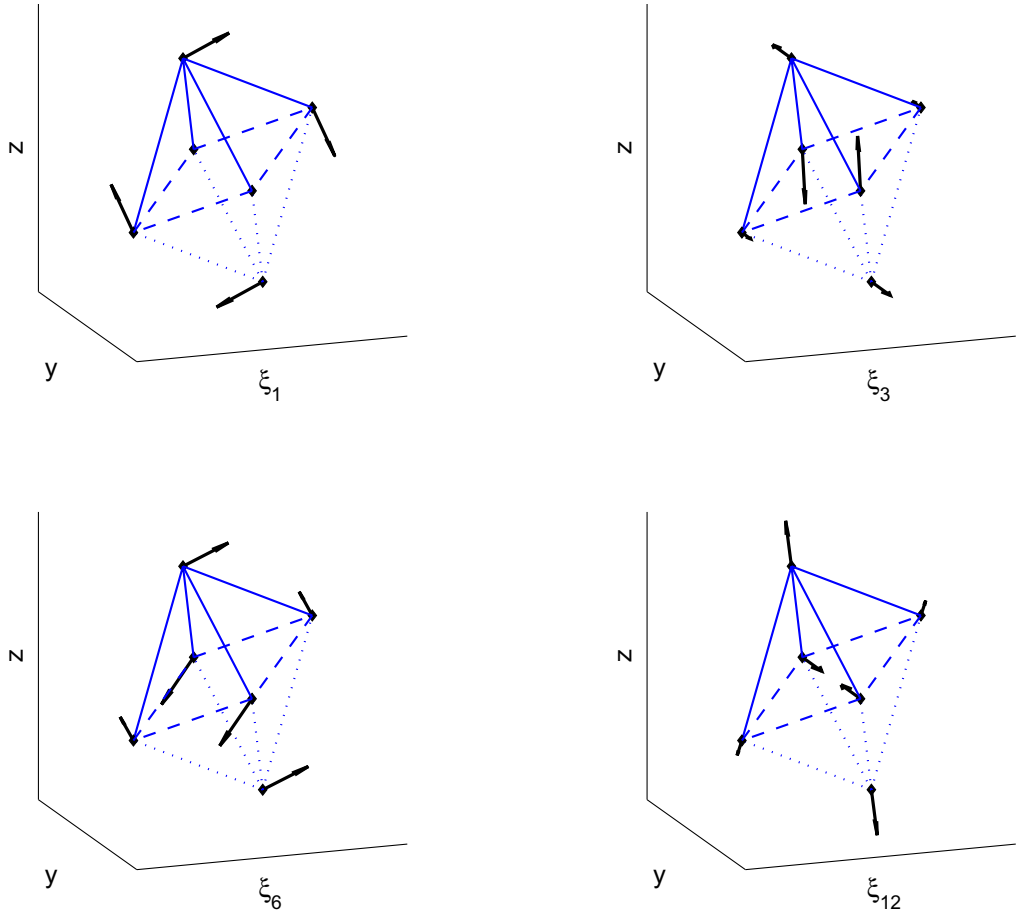

Figure 2. The ions' primary direction of oscillation (given by $\vec{C}_0$), in four Floquet–Lyapunov modes, which are numbered starting from the lowest frequency, with ξ_1 being the lowest-frequency mode.

each coordinate is $q_\alpha/2$ of the respective average position and that in the linear Paul trap, the axial micromotion is negligibly small.

When the crystal solution differs from the pseudopotential limit (as in the peculiar crystals discussed above) or when a very accurate expansion of the modes is desired, the derivation of equation (32) takes into account the full rf crystal solution and ion interactions along the periodic trajectory. Section 4 briefly describes how to solve for the decoupled modes of oscillations of the ions, allowing one to obtain explicitly the mode frequencies and solution vectors.

We have focused on single-species crystals in quadrupole traps, specifically the linear and hyperbolic Paul traps. However, generalization to other cases is easy. Crystals in multipole traps [76–78] can be treated by expanding the motion around a suitable periodic solution $\{\vec{R}_i^{\pi}\}$ as in section 3.3. Keeping only the leading terms will lead to the equations treated above. Segmented traps and trap arrays [79–82] can be handled simply by changing the Mathieu parameters felt by each ion (assuming that the rf drive has an identical frequency). Crystals of nonidentical ions and other types of driving can be treated similarly, and various transformations [83] can be used to handle a more general linear system similar to equation (32),

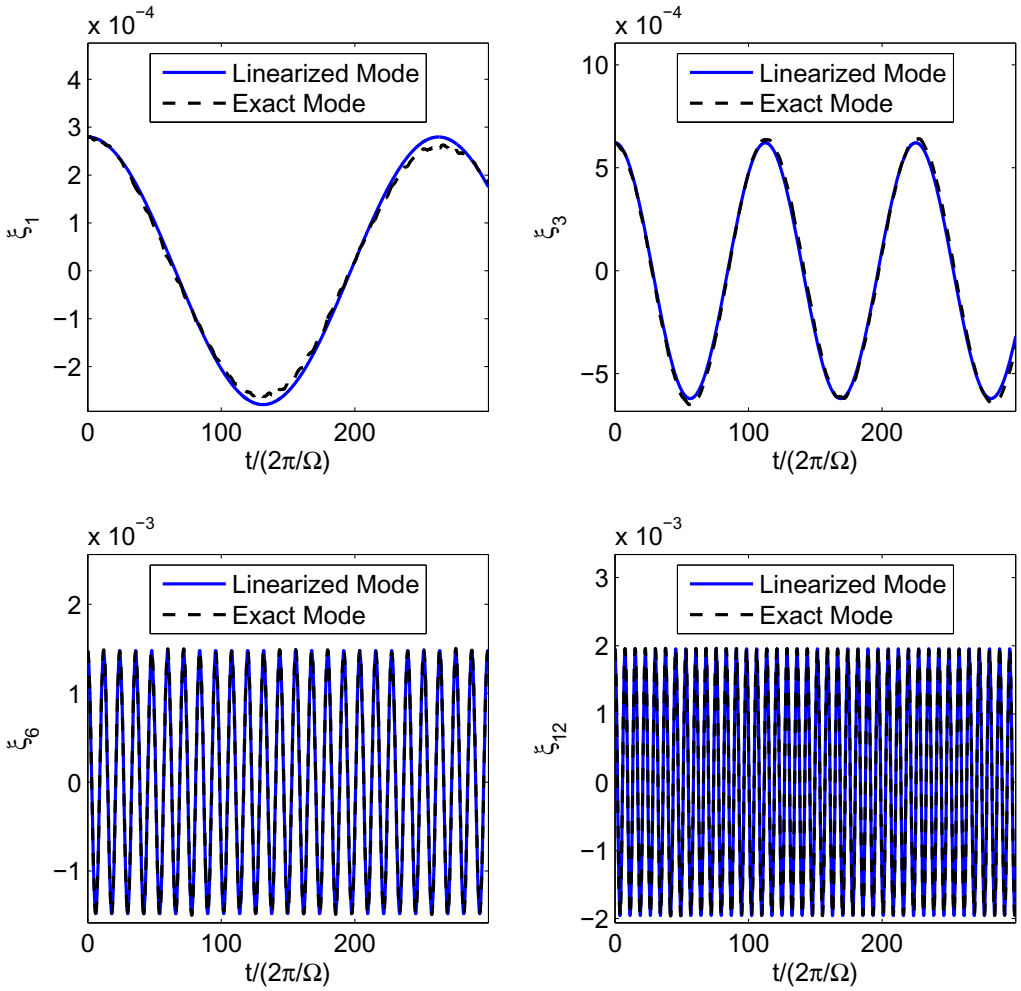

Figure 3. Comparison of the analytical expansion with the exact numerical solution, for the Floquet–Lyapunov modes of figure 2, with small random initial conditions. The modes are numbered starting from the lowest frequency, with ξ_1 being the lowest frequency mode. Time is measured in periods of the rf frequency, and the corresponding natural nondimensional units are used for distances.

such as systems with first-order derivatives (e.g. linear damping, gyroscopic forces or magnetic fields [69, 84]).

The framework presented here for calculating the classical normal modes and their frequencies can find immediate application in most studies involving trapped ion Coulomb crystals, including studies of how ion Coulomb crystals differ from uniformly charged liquid models [14], and possibly even crystalline beams [85, 86]. The analysis is based on linearization of the nonlinear solution about a periodic solution, and the nonlinear correction terms can be written as a series expansion in the Floquet modes about the crystal solution. In a quadrupole trap the nonlinear terms would come only from the Coulomb interaction, and in a multipole trap, there will be terms coming from the nonlinear trapping potential. Such an expansion may

serve as a starting point for the study of nonlinear collective phenomena, e.g. the important phenomenon of rf heating (e.g. [20, 73, 87, 88] and many more).

In addition, an exact quantum description of the modes, and wavefunctions in the configuration space of the ions, is presented in [72] by utilizing the Floquet–Lyapunov transformation described in section 4. The nontrivial time-dependent wavefunctions could, e.g., eventually become important for understanding trapped ion chemistry at ultracold temperatures [89].

Acknowledgments

BR acknowledges support from the Israel Science Foundation and the European Commission (PICC). BR and AR acknowledge support from the the German-Israeli Foundation. MD acknowledges financial support from the Carlsberg Foundation and the EU via the FP7 projects 'Physics of Ion Coulomb Crystals' (PICC) and 'Circuit and Cavity Quantum Electrodynamics' (CCQED). HL thanks R Geffen and M Brownnutt.

References

[1] Major F G, Gheorghe V N and Werth G 2005 *Charged Particle Traps: Physics and Techniques of Charged Particle Field Confinement* (*Springer Series on Atomic, Optical and Plasma Physics* vol 1) (Berlin: Springer)

[2] Werth G, Gheorghe V N and Major F G 2009 *Charged Particle Traps II: Applications* (*Springer Series on Atomic, Optical and Plasma Physics*) (Berlin: Springer)

[3] Gerlich D 2007 *Inhomogeneous RF Fields: A Versatile Tool for the Study of Processes with Slow Ions* (New York: Wiley) pp 1–176

[4] Willitsch S, Bell M T, Gingell A D and Softley T P 2008 Chemical applications of laser- and sympathetically-cooled ions in ion traps *Phys. Chem. Chem. Phys.* **10** 7200–10

[5] Ostendorf A, Zhang C B, Wilson M A, Offenberg D, Roth B and Schiller S 2006 Sympathetic cooling of complex molecular ions to millikelvin temperatures *Phys. Rev. Lett.* **97** 243005

[6] Offenberg D, Zhang C B, Wellers Ch, Roth B and Schiller S 2008 Translational cooling and storage of protonated proteins in an ion trap at subkelvin temperatures *Phys. Rev.* A **78** 061401

[7] Daniilidis N, Narayanan S, Mller S A, Clark R, Lee T E, Leek P J, Wallraff A, Schulz S, Schmidt-Kaler F and Hffner H 2011 Fabrication and heating rate study of microscopic surface electrode ion traps *New J. Phys.* **13** 013032

[8] Metcalf H J and Straten P V 1999 *Laser Cooling and Trapping* (*Graduate Texts in Contemporary Physics*) (Berlin: Springer)

[9] Diedrich F, Peik E, Chen J M, Quint W and Walther H 1987 Observation of a phase transition of stored laser-cooled ions *Phys. Rev. Lett.* **59** 2931–4

[10] Wineland D J, Bergquist J C, Itano W M, Bollinger J J and Manney C H 1987 Atomic-ion Coulomb clusters in an ion trap *Phys. Rev. Lett.* **59** 2935–8

[11] Hasse R W and Avilov V V 1991 Structure and Madelung energy of spherical Coulomb crystals *Phys. Rev.* A **44** 4506–15

[12] Hasse R W and Schiffer J P 1990 The structure of the cylindrically confined Coulomb lattice *Ann. Phys.* **203** 419–48

[13] Schiffer J P 1993 Phase transitions in anisotropically confined ionic crystals *Phys. Rev. Lett.* **70** 818–21

[14] Daniel Dubin H E 1991 Theory of electrostatic fluid modes in a cold spheroidal non-neutral plasma *Phys. Rev. Lett.* **66** 2076–9

[15] Dubin D H E and Schiffer J P 1996 Normal modes of cold confined one-component plasmas *Phys. Rev.* E **53** 5249–67
[16] Dubin D H E 1996 Effect of correlations on the thermal equilibrium and normal modes of a non-neutral plasma *Phys. Rev.* E **53** 5268–90
[17] Totsuji H, Kishimoto T, Totsuji C and Tsuruta K 2002 Competition between two forms of ordering in finite Coulomb clusters *Phys. Rev. Lett.* **88** 125002
[18] Schiffer J P 2002 Melting of crystalline confined plasmas *Phys. Rev. Lett.* **88** 205003
[19] Matthey T, Hansen J P and Drewsen M 2003 Coulomb bicrystals of species with identical charge-to-mass ratios *Phys. Rev. Lett.* **91** 165001
[20] Schiffer J P, Drewsen M, Hangst J S and Hornekr L 2000 Temperature, ordering and equilibrium with time-dependent confining forces. *Proc. Natl Acad. Sci.* **97** 10697–700
[21] Mitchell T B, Bollinger J J, Dubin D H E, Huang X-P, Itano W M and Baughman R H 1998 Direct observations of structural phase transitions in planar crystallized ion plasmas *Science* **282** 1290–3
[22] Itano W M, Bollinger J J, Tan J N, Jelenkovic B, Huang X-P and Wineland D J 1998 Bragg diffraction from crystallized ion plasmas *Science* **279** 686–9
[23] Drewsen M, Brodersen C, Hornekær L, Hangst J S and Schifffer J P 1998 Large ion crystals in a linear Paul trap *Phys. Rev. Lett.* **81** 2878–81
[24] Hornekær L, Kjærgaard N, Thommesen A M and Drewsen M 2001 Structural properties of two-component Coulomb crystals in linear Paul traps *Phys. Rev. Lett.* **86** 1994–7
[25] Kjærgaard N and Drewsen M 2003 Observation of a structural transition for Coulomb crystals in a linear Paul trap *Phys. Rev. Lett.* **91** 095002
[26] Hornekær L and Drewsen M 2002 Formation process of large ion Coulomb crystals in linear Paul traps *Phys. Rev.* A **66** 013412
[27] Drewsen M, Jensen I S, Kjrgaard N, Lindballe J, Mortensen A, Mlhave K and Voigt D 2003 Non-stationary Coulomb crystals in linear Paul traps *J. Phys. B: At. Mol. Opt. Phys.* **36** 525
[28] Retzker A, Thompson R C, Segal D M and Plenio M B 2008 Double well potentials and quantum phase transitions in ion traps *Phys. Rev. Lett.* **101** 260504
[29] Dantan A, Marler J P, Albert M, Guénot D and Drewsen M 2010 Noninvasive vibrational mode spectroscopy of ion Coulomb crystals through resonant collective coupling to an optical cavity field *Phys. Rev. Lett.* **105** 103001
[30] Rosenband T *et al* 2008 Frequency ratio of Al^+ and Hg^+ single-ion optical clocks; metrology at the 17th decimal place *Science* **319** 1808–12
[31] Herskind P F, Dantan A, Marler J P, Albert M and Drewsen M 2009 Realization of collective strong coupling with ion Coulomb crystals in an optical cavity *Nature Phys.* **5** 494–8
[32] Albert M, Dantan A and Drewsen M 2011 Cavity electromagnetically induced transparency and all-optical switching using ion Coulomb crystals *Nature Photon.* **5** 633–6
[33] Home J P, Hanneke D, Jost J D, Amini J M, Leibfried D and Wineland D J 2009 Complete methods set for scalable ion trap quantum information processing *Science* **325** 1227–30
[34] Mølhave K and Drewsen M 2000 Formation of translationally cold MgH^+ and MgD^+ molecules in an ion trap *Phys. Rev.* A **62** 011401
[35] Staanum P F, Højbjerre K, Skyt P S, Hansen A K and Drewsen M 2010 Rotational laser cooling of vibrationally and translationally cold molecular ions *Nature Phys.* **6** 271–4
[36] Schneider T, Roth B, Duncker H, Ernsting I and Schiller S 2010 All-optical preparation of molecular ions in the rovibrational ground state *Nature Phys.* **6** 275–8
[37] Mortensen A, Nielsen E, Matthey T and Drewsen M 2006 Observation of three-dimensional long-range order in small ion Coulomb crystals in an rf trap *Phys. Rev. Lett.* **96** 103001
[38] Diedrich F, Bergquist J C, Itano W M and Wineland D J 1989 Laser cooling to the zero-point energy of motion *Phys. Rev. Lett.* **62** 403–6

[39] Roos Ch, Zeiger Th, Rohde H, Nägerl H C, Eschner J, Leibfried D, Schmidt-Kaler F and Blatt R 1999 Quantum state engineering on an optical transition and decoherence in a Paul trap *Phys. Rev. Lett.* **83** 4713–6
[40] King B E, Wood C S, Myatt C J, Turchette Q A, Leibfried D, Itano W M , Monroe C and Wineland D J 1998 Cooling the collective motion of trapped ions to initialize a quantum register *Phys. Rev. Lett.* **81** 1525–8
[41] Mortensen A, Nielsen E, Matthey T and Drewsen M 2007 Radio frequency field-induced persistent long-range ordered structures in two-species ion Coulomb crystals *J. Phys. B: At. Mol. Opt. Phys.* **40** F223
[42] Wuerker R F, Shelton H and Langmuir R V 1959 Electrodynamic containment of charged particles *J. Appl. Phys.* **30** 342–9
[43] Bluemel R, Chen J M, Peik E, Quint W, Schleich W, Shen Y R and Walther H 1988 Phase transitions of stored laser-cooled ions *Nature* **334** 309–13
[44] Hoffnagle J, DeVoe R G, Reyna L and Brewer R G 1988 Order-chaos transition of two trapped ions *Phys. Rev. Lett.* **61** 255–8
[45] Blümel R, Kappler C, Quint W and Walther H 1989 Chaos and order of laser-cooled ions in a Paul trap *Phys. Rev.* A **40** 808–23
[46] Brewer R G, Hoffnagle J and DeVoe R G 1990 Transient two-ion chaos *Phys. Rev. Lett.* **65** 2619–22
[47] Baumann G and Nonnenmacher T F 1992 Regular and chaotic motions in ion traps: a nonlinear analysis of trap equations *Phys. Rev.* A **46** 2682–92
[48] Farrelly D and Howard J E 1993 Comment on 'regular and chaotic motions in ion traps: a nonlinear analysis of trap equations' *Phys. Rev.* A **48** 851–3
[49] Blümel R 1993 Comment on 'regular and chaotic motions in ion traps: a nonlinear analysis of trap equations' *Phys. Rev.* A **48** 854–5
[50] Baumann G and Nonnenmacher T F 1993 Reply to comments on 'regular and chaotic motions in ion traps: a nonlinear analysis of trap equations' *Phys. Rev.* A **48** 856–7
[51] Hoffnagle J and Brewer R G 1993 Frequency-locked motion of two particles in a Paul trap *Phys. Rev. Lett.* **71** 1828–31
[52] Hoffnagle J and Brewer R G 1994 On the frequency-locked orbits of two particles in a Paul trap *Science* **265** 213–5
[53] Hoffnagle J and Brewer R G 1994 Chaotic transients of two particles in a Paul trap: interpretation as a boundary crisis *Phys. Rev.* A **50** 4157–69
[54] Shen J-L, Yin H-W, Dai J-H and Zhang H-J 1997 Dynamical behavior, transient chaos and riddled basins of two charged particles in a Paul trap *Phys. Rev.* A **55** 2159–64
[55] Emmert J W, Moore M and Blümel R 1993 Prediction of a deterministic melting transition of two-ion crystals in a Paul trap *Phys. Rev.* A **48** R1757–60
[56] Moore M G and Blümel R 1994 Prediction of an alignment transition region of two-ion crystals in a Paul trap *Phys. Rev.* A **50** R4453–6
[57] Moore M G and Blümel R 1995 An improved pseudo potential for the two-ion Paul trap *Phys. Scr.* **1995** 429
[58] Hoffnagle J A and Brewer R G 1995 Stability of two-ion crystals in the Paul trap: a comparison of exact and pseudopotential calculations *Appl. Phys.* B **60** 113–7
[59] Drewsen M and Brøner A 2000 Harmonic linear Paul trap: stability diagram and effective potentials *Phys. Rev.* A **62** 045401
[60] Vogt A W 1994 Nonlinear resonances and the melting of Wigner crystals in a Paul trap *Phys. Rev.* A **49** R657–60
[61] Vogt A W 1994 Nonlinear resonances and phase transitions of two-ion Coulomb clusters in a Paul trap: calculations without laser cooling *Appl. Phys.* B **58** 57–62
[62] Garrick-Bethell I, Clausen Th and Blümel R 2004 Universal instabilities of radio-frequency traps *Phys. Rev.* E **69** 056222
[63] Koštrun M, Smith W W and Javanainen J 1998 Theory of the π-periodic motion of two ions in a Paul trap *Phys. Rev.* A **57** 2895–04

[64] Leibfried D, Blatt R, Monroe C and Wineland D 2003 Quantum dynamics of single trapped ions *Rev. Mod. Phys.* **75** 281–324
[65] Ghosh P K 1995 *Ion Traps* (Oxford: Clarendon)
[66] McLachlan N W 1947 *Theory and Applications of Mathieu Functions* (Oxford: Clarendon)
[67] Kjærgaard N, Mølhave K and Drewsen M 2002 Stability of Coulomb crystals in a linear Paul trap with storage-ring-like confinement *Phys. Rev.* E **66** 015401
[68] Kjærgaard N and Drewsen M 2003 Observation of a structural transition for Coulomb crystals in a linear Paul trap *Phys. Rev. Lett.* **91** 095002
[69] Piacente G, Schweigert I V, Betouras J J and Peeters F M 2004 Generic properties of a quasi-one-dimensional classical Wigner crystal *Phys. Rev.* B **69** 045324
[70] Morigi G and Fishman S 2004 Eigenmodes and thermodynamics of a Coulomb chain in a harmonic potential *Phys. Rev. Lett.* **93** 170602
[71] Morigi G and Fishman S 2004 Dynamics of an ion chain in a harmonic potential *Phys. Rev.* E **70** 066141
[72] Landa H, Drewsen M, Reznik B and Retzker A 2012 Classical and quantum modes of coupled Mathieu equations arXiv:1206.0716
[73] Zhang C B, Offenberg D, Roth B, Wilson M A and Schiller S 2007 Molecular-dynamics simulations of cold single-species and multispecies ion ensembles in a linear Paul trap *Phys. Rev.* A **76** 012719
[74] Apolinario S W S, Partoens B and Peeters F M 2007 Structural and dynamical aspects of small three-dimensional spherical Coulomb clusters *New J. Phys.* **9** 283
[75] Bonitz M, Henning C and Block D 2010 Complex plasmas: a laboratory for strong correlations *Rep. Prog. Phys.* **73** 066501
[76] Okada K, Yasuda K, Takayanagi T, Wada M, Schuessler H A and Ohtani S 2007 Crystallization of Ca^+ ions in a linear rf octupole ion trap *Phys. Rev.* A **75** 033409
[77] Okada K, Takayanagi T, Wada M, Ohtani S and Schuessler H A 2009 Observation of ion Coulomb crystals in a cryogenic linear octupole rf ion trap *Phys. Rev.* A **80** 043405
[78] Champenois C, Marciante M, Pedregosa-Gutierrez J, Houssin M, Knoop M and Kajita M 2010 Ion ring in a linear multipole trap for optical frequency metrology *Phys. Rev.* A **81** 043410
[79] Allcock D T C *et al* 2010 Implementation of a symmetric surface-electrode ion trap with field compensation using a modulated Raman effect *New J. Phys.* **12** 053026
[80] Kumph M, Brownnutt M and Blatt R 2011 Two-dimensional arrays of radio-frequency ion traps with addressable interactions *New J. Phys.* **13** 073043
[81] Welzel J, Bautista-Salvador A, Abarbanel C, Wineman-Fisher V, Wunderlich C, Folman R and Schmidt-Kaler F 2011 Designing spin–spin interactions with one and two dimensional ion crystals in planar micro traps *Eur. Phys. J. D: At. Mol. Opt. Plasma Phys.* **65** 285–97
[82] Ravi K, Lee S, Sharma A, Ray T, Werth G and Rangwala S A 2010 Three-dimensional lattice of ion traps *Phys. Rev.* A **81** 031401
[83] Yakubovich V A and Starzhinskii V M 1975 *Linear Differential Equations with Periodic Coefficients* (New York: Wiley)
[84] Baltrusch J D, Negretti A, Taylor J M and Calarco T 2011 Fast and robust quantum computation with ionic Wigner crystals *Phys. Rev.* A **83** 042319
[85] Schätz T, Schramm U and Habs D 2001 Crystalline ion beams *Nature* **412** 717–20
[86] Li X-P, Enokizono H, Okamoto H, Yuri Y, Sessler A M and Wei J 2006 Phonon spectrum and the maintenance condition of crystalline beams *Phys. Rev. ST Accel. Beams* **9** 034201
[87] Ryjkov V L, Zhao X Z and Schuessler H A 2005 Simulations of the rf heating rates in a linear quadrupole ion trap *Phys. Rev.* A **71** 033414
[88] Buluta I M, Kitaoka M, Georgescu S and Hasegawa S 2008 Investigation of planar Coulomb crystals for quantum simulation and computation *Phys. Rev.* A **77** 062320
[89] Carr L D, DeMille D, Krems R V and Ye J 2009 Cold and ultracold molecules: science, technology and applications *New J. Phys.* **11** 055049